Geofísica Internacional (2018) 57-1: 39-58

Original paper

Estimation of ground subsidence in the city of Morelia, Mexico using Satellite Interferometry (INSAR)s

Gerardo Suárez, Said H. Jaramillo, Penélope López-Quiroz and Osvaldo Sánchez-Zamora

Received: June 07, 2017 ; accepted: October 19, 2017; published on line: January 01, 2018

Resumen

La ciudad de Morelia, en la zona central de México, ha sido afectada en años recientes por la subsidencia diferencial del suelo que se refleja en forma de fallas y fracturas en la superficie. El objetivo de este trabajo es el obtener series de tiempo de la deformación del suelo utilizando interferogramas InSAR, con el fin de determinar la evolución espacial y temporal de la subsidencia en la ciudad de Morelia. Con este fin se procesaron 28 imágenes de ENVISAT-ASAR, adquiridas de mayo de 2003 a septiembre de 2010. Se limitaron las lineas de base perpendiculares y temporales a ser menos de 400 m y 420 días respectivamente, como un criterio de calidad para seleccionar los interferogramas. De un total de 378 interferogramas, se consideró que únicamente 65 tenían la suficiente calidad para ser usados en la inversión, basado en la decorrelación obervada en las señales. Los resultados muestran que la mayor parte de la ciudad de Morelia no está afectada por subsidencia del suelo de manera significativa. En areas donde si hay subsidencia del terreno, las velocidades varían de 0.7 a 5 cm/año. La mayor subsidencia se da en forma de estructuras circulares y a lo largo de algunas de las fallas observadas en la superficie. La subsidencia del terreno está concentrada en áreas específicas al pie de la fallas La Colina, Central Camionera y La Paloma. Sin embargo, la subsidencia no es continua a lo largo de estas fallas y se observa únicamente en segmentos especificos de las mismas. En algunos casos, como por ejemplo la falla La Paloma, la subsidencia parece estar asociada con fuertes cambios litológicos entre el techo y el piso de las fallas. En otros casos, como en las fallas Central Camionera y La Colina, la subsidencia diferencial observada parece estar asociada a la compleja estructura del basamento y del subsuelo de la ciudad de Morelia, y relacionada primordialmente con la compactación diferencial de los sedimentos de la cuenca.

Palabras clave: Subsidencia del terreno, interferometría, InSAR, Morelia, México, extracción de aguas subterráneas

G. Suárez
O. Sánchez-Zamora
Instituto de Geofísica
Universidad Nacional Autónoma de México
Ciudad Universitaria
Delegación Coyoacán 04510
México CDMX, México
*Corresponding author:

S. H. Jaramillo
Posgrado en Ciencias de la Tierra
Instituto de Geofísica
Universidad Nacional Autónoma de México
Ciudad Universitaria
Delegación Coyoacán 04510
México CDMX, México

P. López-Quiroz
Centro de Geociencias
Universidad Nacional Autónoma de México
Querétaro, México

Abstract

In recent years, the city of Morelia, in central Mexico, has been affected by differential subsidence of the soil evidenced by faults and fractures on the ground. The goal of this study is to obtain ground deformation time series from InSAR interferograms, in order to determine the temporal and spatial evolution of subsidence in the city of Morelia. Twenty-eight ENVISAT-ASAR images, acquired from May 2003 to September 2010, were processed. Perpendicular and temporal baselines of less than 400 m and 420 days respectively, were used as criteria to select interferograms. From a total of 378 interferograms, only 65 were considered to be of sufficient quality, based on the observed signal decorrelation. The results show that most of the city of Morelia is not affected by significant subsidence. In the areas where subsidence occurs, the rates of subsidence vary between 0.7 and 5 cm/yr. Most of the subsidence is in the form of discrete circular patterns and along segments of the observed surface faults. Ground subsidence is concentrated in specific areas on the footwalls of La Colina, Central Camionera and La Paloma faults. Subsidence, however, is not continuous along these faults, but observed only in some segments. In some cases, as in the case of La Paloma fault, the subsidence appears to be directly associated with the strong lithological contrast between the footwall and the hanging wall. In the other two cases, such as the Central Camionera and La Colina faults, the differential subsidence observed appears to be related with the complex basement and sedimentary structure of the volcanic subsoil of the city of Morelia and related primarily to differential compaction of the sedimentary fill.

Key words: Ground subsidence, interferometry, InSAR, Morelia, Mexico, ground water extraction.

Introduction

The subsidence of sedimentary basins is a process that affects many cities worldwide (*e.g*., Amelung *et al*., 1999; Buckley *et al*., 2003; Chai *et al*., 2004; Dehghani *et al*., 2009; Ding *et al*., 2004; Le Mouélic *et al*., 2005; Lu and Liao, 2008; Marfai and King, 2007; Stramondo *et al*., 2008; Strozzi *et al*., 2001; Vilardo *et al*., 2009; Watson *et al*., 2002). In general, differential ground subsidence in urban areas is related to the withdrawal of groundwater to meet human, industrial and agricultural needs (Poland, 1984). The over-exploitation of the aquifers decreases the pore pressure and induces the compaction of the sediments as a result of the inelastic deformation of the aquitard (Amelung *et al*., 1999).

The firsts cases of differential subsidence in Mexico due to water extraction were observed in Mexico City in the early 1920s (Gayol, 1925). Subsidence increased rapidly from 1930 to 1960 due to the rapid growth of the population (Ortega-Guerrero *et al*., 1993). Carrillo (1948) was the first to relate directly the subsidence with the over-exploitation of the aquifers in Mexico City. In the 1980s, differential subsidence began to be observed and documented in several cities in central Mexico, such as: Aguascalientes, Morelia, Celaya, Irapuato, Salamanca, Querétaro, Toluca and San Luis Potosí (*e.g*., Aguirre-Díaz *et al*., 2000; Ávila-Olivera, 2008; Ávila-Olivera *et al*., 2010; Ávila-Olivera and Garduño-Monroy, 2006; Calderhead *et al*., 2011; Carreón-Freyre and Cerca, 2006; Castañeda *et al*., 1993, 1995; Chávez-Alegría, 2008; Cigna *et al*., 2011; 2012; Esquivel, 2009; Farina *et al*., 2007, 2008; Garduño-Monroy *et al*., 2001; López-Doncel *et al*., 2006; Mejía-Gómez and Sandoval-Minero, 2004; Pacheco-Martínez; 2007; Pacheco-Martínez and Arzate-Flores, 2007; Pacheco-Martínez *et al*., 2006; Schroeder-Aguirre, 2010; Trujillo-Candelaria, 1989, 2009; Vargas, 1999; Zermeño de León *et al*., 2004, 2005;).

More recently, interferometric techniques were used to study the rapid subsidence of Mexico City and its suburbs (e.g., Strozzi and Wegmüller, 1999; Strozzi *et al*., 2001; Carreón-Freyre *et al*., 2006; Cabral-Cano *et al*., 2008; López-Quiroz, 2008; López-Quiroz *et al*. 2009; Osmanolu *et al*., 2011). The common denominator shared by these cities is their location on lacustrine and fluvial-lacustrine basins filled with sediments that are heterogeneous in both composition and structure.

In the particular case of the city of Morelia, discussed in this paper, subsidence of the ground was first recognized in 1983, coinciding with the rapid increase of the urban population (Arreygue-Rocha *et al*., 2002; 2005). The differential subsidence was manifested on the surface as soil fractures damaging houses and buildings in the urban area (*e.g*., Garduño-Monroy *et al*., 2001; Ávila-Olivera and

Garduño-Monroy, 2006; Ávila-Olivera, 2008). The Central Camionera and La Colina faults were the first physiographic features identified as resulting from the differential subsidence of the ground (Figure 1). The rates of subsidence reported from *in situ* measurements range from 4 to 6 cm/yr (Garduño-Monroy *et al*., 2001). To our knowledge, no routine and repeated measurement of ground deformation are done in the city.

Several faults affecting the city of Morelia have been mapped: La Paloma, La Colina, Central Camionera, Cuautla, Torremolinos, El Realito, La Soledad, Chapultepec and Ventura Puente (Ávila-Olivera, 2008; Ávila-Olivera and Garduño-Monroy, 2008; Cabral-Cano *et al*., 2010; Cigna *et al*., 2012) (Figure 1). The orientation of these faults is predominantly NE-SW and E-W. Several authors proposed that these faults are parallel to the mapped regional tectonic faults (Ávila-Olivera, 2008; Ávila -Olivera and Garduño-Monroy, 2006; Farina *et al*., 2007; 2008; Garduño-Monroy *et al*., 2001). Furthermore, Garduño-Monroy *et al*., (2001) suggested that La Colina and La Paloma faults are the surface expression of motion on basement faults of tectonic origin.

The early studies that measured subsidence in the city of Morelia using InSAR were based on interferograms produced using only images pairs (Table 1). More recently, Cabral-Cano *et al*. (2010) and Cigna *et al*. (2012) used the method of persistent scatterers (PSI) (Ferreti *et al*., 2000; 2001) to obtain time series of the subsidence at specific locations. Chaussard *et al*., (2014) used the Small Baselines (SBAS) methodology on ALOS images to estimate average subsidence in the city. Here, we extend the work of Cigna *et al*. (2012) using the method of SBAS (Berardino *et al*., 2002; Schmidt and Bürgmann, 2003; Usai, 2003; Cavalié *et al*., 2007; López-Quiroz *et al*., 2009) to obtain time series of the subsidence across several cross sections and specific locations. The purpose of applying this technique was to increase the signal coherence and to minimize its temporal and spatial decorrelation (Berardino *et al*., 2002; Yan *et al*., 2009). The use of this method allowed us to obtain reliable time series that reflect the evolution of the ground deformation as a function of time, induced by subsidence of the soil in Morelia.

InSAR processing

Twenty-eight ENVISAT-ASAR images, acquired from May 2003 to September 2010, were processed using the software *JPL/CalTech Repeat Orbit Interferometry Package (ROI_PAC)* (Rosen *et al*., 2004). *ROI_PAC* was used to

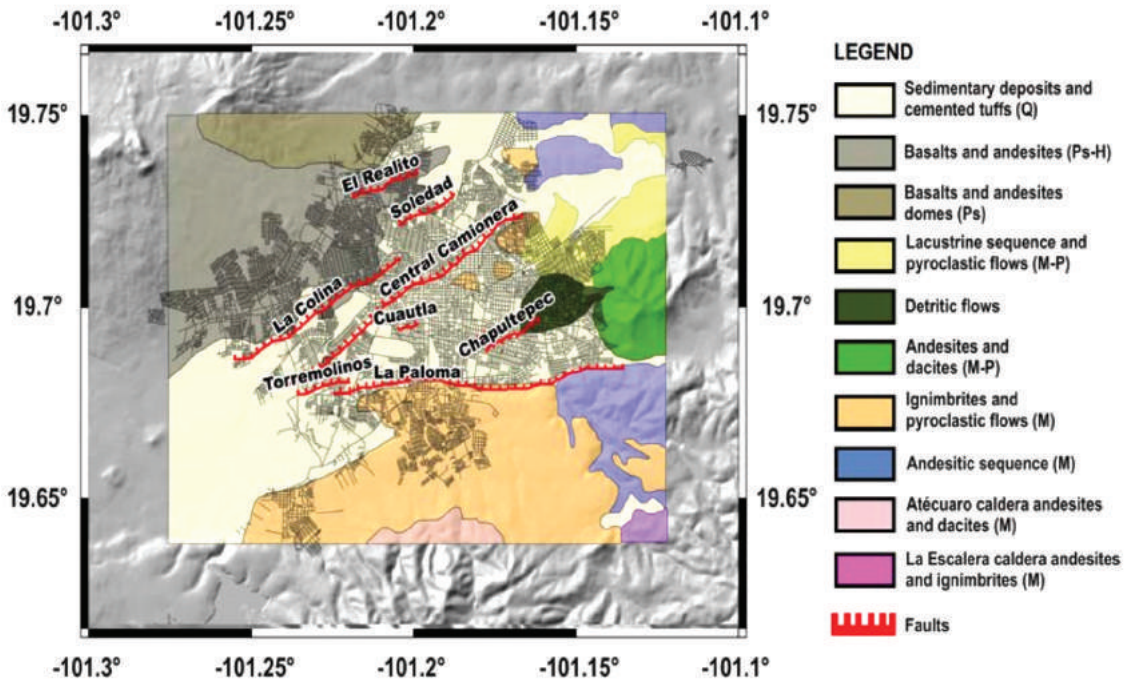

Figure 1. Geological setting and location of the main faults that affect the city of Morelia in Michoacán, México (modified from Cigna *et al*., 2012). Abbreviations: Q-Quaternary; Ps-Pleistocene; H-Holocene; M-Miocene.

Table 1. Analyses carried out in Morelia using InSAR.

Author	Method	Interferograms spanning time	Subsidence [mm/yr]
Farina *et al*. (2007)	DInSAR[1]	July 2003 – November 2004 December 2004- December 2005	10-35
Ávila-Olivera (2008)	DInSAR[1]	July 2003 – November 2004 December 2004- December 2005	10
Farina *et al*. (2008)	DInSAR[1]	July 2003 – November 2004 December 2004- December 2005	10-35
Ávila-Olivera *et al*. (2010)	DInSAR[1]	July 2003 – November 2004	35
Cabral-Cano *et al*. (2010)	PSI[2]	July 2003 – October 2009	50
Cigna *et al*. (2011)	PSI[2]	July 2003 – October 2009	50
Cigna *et al*. (2012)	DInSAR[1] PSI[2]	July 2003 – May 2009	70-80 40-50

[1] DInSAR – Differential Interferometry
[2] PSI: Permanent Scatterer Interferometry

construct and to unwrap the interferograms. All scenes are descending-orbit images (track 69, frame 3213). The orbital fringes were removed using the satellite orbital corrections provided by the Department of Earth Observation and Space Systems (*DEOS*) of Delft University of Technology and by the European Space Agency (*ESA*). The topographic contribution was corrected using a 1" arc, digital elevation model (DEM) resampled from the 3" arc DEM of the Shuttle Radar Topography Mission (*SRTM*) (Farr and Kobrick, 2000). Multilooking by a factor of five was applied in the direction of azimuth. This process leads to a ground pixel resolution of ~20 x 20 m. In order to increase the signal to noise ratios, a nonlinear adaptive spatial filtering (Goldstein and Werner, 1998) was applied to all interferograms. As described below in more detail, the interferograms were unwrapped using the branch-cut algorithm (Goldstein *et al*., 1988).

In order to avoid loss of coherence in the interferograms, their baselines were limited to 1) spatial perpendicular baselines of less than 400 m; and 2) temporal baselines of less than 420 days. As a result, 65 interferograms were selected, constituting two separate groups (Figure 2). The first one spans from July 2003 to January 2007, and the second from December 2008 to September 2010. Unfortunately there are no InSAR acquisitions in the region from February 2007 to November 2008. Usai (2003) proposed to overcome large gaps in the interferometric data by creating synthetic interferograms that predict a particular deformation behavior. However, the period missing is very long to select *a priori* a reliable behavior. Therefore, the two observational periods are treated as independent groups.

Atmospheric phase delays due to the vertical stratification of the atmosphere (Hanssen, 2001) and to the orbital inaccuracies, for which we estimate the best fitting 'twisted plane' (Cavalié *et al*., 2007), were calculated simultaneously following López-Quiroz *et al*. (2009). The corrected interferograms were co-registered prior to the inversion process. The phase delay time series were obtained using a least-squares inversion (*e.g.,* Cavalié *et al*., 2007). The mean square errors (RMS) of all interferograms and pixels were calculated in order to detect unwrapping errors and inconsistencies in the interferometric dataset (Appendix A).

Finally, average subsidence rates were calculated as a function of time for all pixels meeting the following criteria: 1) To have the complete number of acquisitions and; 2) To show an RMS error of less than 0.5 rad. All analyses were performed in radar geometry and later geo-referenced to the DEM.

Description of the inversion process

As suggested by Schmidt and Bürgmann (2003), the inversion process was performed without smoothing in order to avoid aliasing effects. The names of the interferograms are identified by the year, month and day of the images used

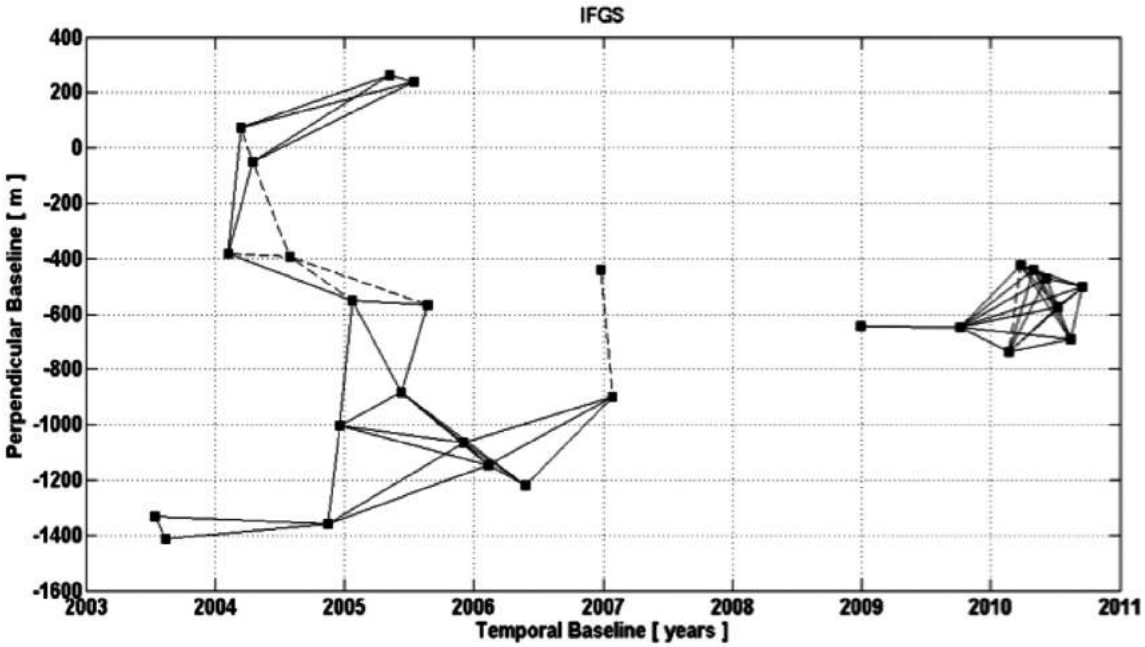

Figure 2. The squares represent the 28 InSAR images obtained for the city of Morelia from 2003 to 2010, plotted as a function of the acquisition date. The solid lines represent the 55 interferograms utilized during the inversion process. The dashed lines represent the 10 interferograms discarded in the inversion process.

to calculate them. Interferograms 20040313-20040417, 20061223-20070127, 20100220-20100327, 20100327-20100501, 20100327-20100605, and 20100501-20100605 were discarded because they did not meet the quality criteria described before. Furthermore, all interferograms sharing the common image 20040731 (20040207-20040731, 20040417-20040731, 20040731-20050122, 20040731-2050820) were not included in the analysis due to the strong atmospheric effects observed in that particular scene, which greatly increased the RMS errors.

Fifty-five interferograms were used in the analysis (Tables 2 and 3). The RMS values of the interferograms used to evaluate the time series are described in equations 2 and 5 in Appendix A and graphically shown on Figure 3.

Discussion of results

Regional ground subsidence in Morelia

The results of the analysis of the two independent time series show that, on a regional scale, most of the urban sprawl of Morelia is not affected by significant ground subsidence (Figures 4a and 4b). During the seven years studied, the average surface deformation was ±0.5 cm/yr. These values are within the error of the methodology. The areas showing subsidence occur on the footwall of some of the mapped faults. The subsidence, however, is not continuous along the whole length of the faults. Subsidence is concentrated in the western part of the city and on specific segments of La Paloma, Central Camionera and La Colina faults. The areas showing ground deformation are consistently the same in the two time series spanning this ten-year period, indicating that the subsidence is consistent in time and areal extent (Figures 4a and 4b). However, our results show a small general increase in the subsidence rate of the affected areas from December 2008 to September 2010, relative to the one observed from July 2003 to January 2007 (Figures 4a and 4b). Cigna *et al*. (2012) observed also this increase in subsidence in the latter years.

Although La Paloma fault represents one of the starker lithological contacts in the city, between the Miocene ignimbrite sequence of the Sierra Mil Cumbres and the basin fill formed by Quaternary sedimentary deposits and cemented tuffs (Figure 1), subsidence is observed mostly in the western end of the fault (Figures 4a and 4b). In this area of La Paloma fault, the zones that were mostly affected by a rapid rate of subsidence are residential areas in the southwestern part of the city: *INFONAVIT Villa Universidad, Valle Quieto, Arboledas,* and *Residencial del Sur.*

Table 2. Interferograms corresponding to the time series July 2003 to January 2007.

ID[1]	Interferogram[1]	B_t[2] [days]	B_D[3] [m]	ID[1]	Interferogram[1]	B_t[2] [days]	B_D[3] [m]
1	20030712-20030816	35	-83	16	20041218-20051203	350	-63
2*	20030712-20041113	490	-28	17	20041218-20060211	420	-141
3*	20030816-20041113	455	55	18	20050122-20050611	140	-335
4*	20040207-20040313	35	457	19	20050122-20050820	210	-16
5	20040207-20040417	70	335	20	20050607-20050716	70	-23
6	20040207-20050122	350	-167	21	20050611-20050820	70	319
7	20040313-20050507	420	188	22	20050611-20051203	175	-182
8[1]	20040313-20050716	490	165	23	20050611-20060211	245	-260
9	20040417-20050507	385	310	24	20050611-20060527	350	-335
10[1]	20040417-20050716	455	287	25	20051203-20060211	70	-78
11	20041113-20041218	35	355	26	20051203-20060527	175	-153
12	20041113-20051203	385	292	27	20051203-20070127	420	166
13[1]	20041113-20060211	455	214	28	20060211-20060527	105	-75
14	20041218-20050122	35	454	29	20060211-20070127	350	244
15	20041218-20050611	175	119	30	20060527-20070127	245	319

[1] Interferogram number. The interferogram was built using the satellite image pairs expressed as year, month and day. The asterisk indicates the interferogram did not meet the prescribed quality criteria.
[2] B_t is the temporal baseline between subsequent radar images
[3] B_D is the spatial perpendicular baseline between subsequent radar images

Table 3. Interferograms corresponding to the time series December 2008 – September 2010.

ID[1]	Interferogram[1]	B_t[2] [days]	B_D[3] [m]	ID[1]	Interferogram[1]	B_t[2] [days]	B_D[3] [m]
1	20081227-20091003	280	-1	14	20100327-20100710	105	-150
2	20091003-20100220	140	-90	15	20100327-20100814	140	-266
3	20091003-20100327	175	224	16	20100327-20100918	175	-79
4	20091003-20100501	210	207	17	20100501-20100710	70	-133
5	20091003-20100605	245	178	18	20100501-20100814	105	-249
6	20091003-20100710	280	74	19	20100501-20100918	140	-62
7	20091003-20100814	315	-42	20	20100605-20100710	35	-104
8	20091003-20100918	350	145	21	20100605-20100814	70	-220
9	20100220-20100501	70	297	22	20100605-20100918	105	-33
10	20100220-20100605	105	268	23	20100710-20100814	35	-116
11	20100220-20100710	140	164	24	20100710-20100918	70	71
12	20100220-20100814	175	48	25	20100814-20100918	35	187
13	20100220-20100918	210	235				

[1] Interferogram number. The interferogram was built using the satellite image pairs expressed as year, month and day.
[2] B_t is the temporal baseline between subsequent radar images
[3] B_D is the spatial perpendicular baseline between subsequent radar images

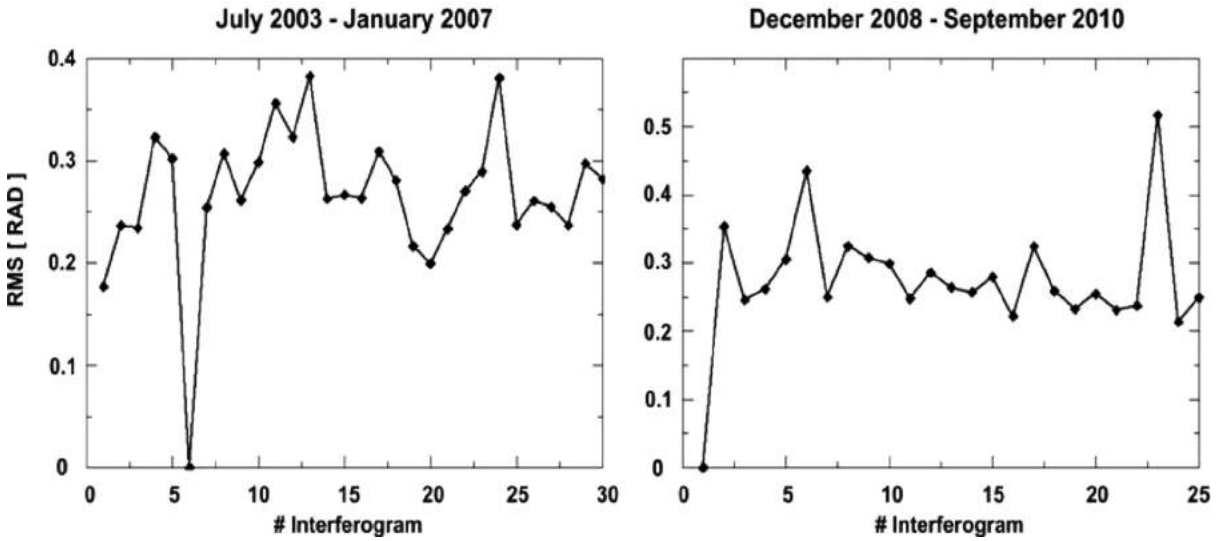

Figure 3. RMS values of the individual interferograms used in the final inversion process.

In the central part of the city of Morelia, the Chapultepec and Cuautla faults show no evidence of ground deformation during the seven years of observation (Figures 1, 4a and 4b). Both time series indicate that no discernable subsidence takes place near these faults during the observation period (Figures 4a and 4b). Farther to the north, the Central Camionera fault reflects rapid subsidence in the central part, gradually tapering off towards the west. The eastern Central Camionera fault shows no evidence of subsidence. The relatively rapid subsidence observed in the central segment of the Central Camionera fault affects the neighborhoods of *El Porvenir, Ampliacion Porvenir* and *Las Flores*.

La Colina fault, to the northwest of the city, reflects the geological boundary between the Pliocene basalts and andesites and the sediment fill of Quaternary age (Figure 1). The footwall of La Colina fault reflects subsidence along its whole length (Figures 4a and 4b). Comparing the two periods analyzed, the largest increase in the rate of subsidence took place along the eastern end of La Colina fault from December 2008 to September 2010 (Figure 4b). Subsidence on La Colina fault affects the housing units of *INFONAVIT Adolfo López Mateos, Las Águilas, Agua Clara,* and the neighborhoods *La Quemada, Irrigacion* and *Vicente Guerrero*.

Cigna *et al*. (2012) did not report a correlation between the ground subsidence in the city and the rate of water extraction and the decrease of the static level of the water wells. In the same manner, a comparison of the ground subsidence with the thickness of the Quaternary deposits showed no relation to the areas of high subsidence rates. Our results confirm the observations made by Cigna *et al*. (2012), suggesting that the subsidence is not directly and exclusively controlled by the thickness of the sediments or by the water extraction rates. The variables controlling the subsidence of the ground appear to be the complex structural distribution of the volcanic deposits forming the Morelia basin and the preexisting basement topography.

Subsidence time series and cross sections in the areas of higher subsidence

As mentioned above, we use the method of Small Baselines (SBAS) (Berardino *et al*., 2002; Schmidt and Bürgmann, 2003; Usai, 2003; Cavalié *et al*., 2007; López-Quiroz *et al*., 2009) in order to extend the work of Cigna *et al*. (2012). The use of this method allowed us to obtain reliable time series that reflect the evolution of the deformation induced by the subsidence in Morelia. Based on this approach, time series of the ground deformation were estimated across several cross sections of the faults. Also, rates of subsidence as a function of time were obtained for several locations in the city (Figures 4a, 4b and 5).

In order to construct the time series and the cross sections, only pixels that met the criteria of having a RMS < 0.5 rad were selected (see Equation 3 in Appendix A). In addition, the selected pixels had to be present in all interferograms. These criteria guarantee a reliable depiction of the behavior and velocity

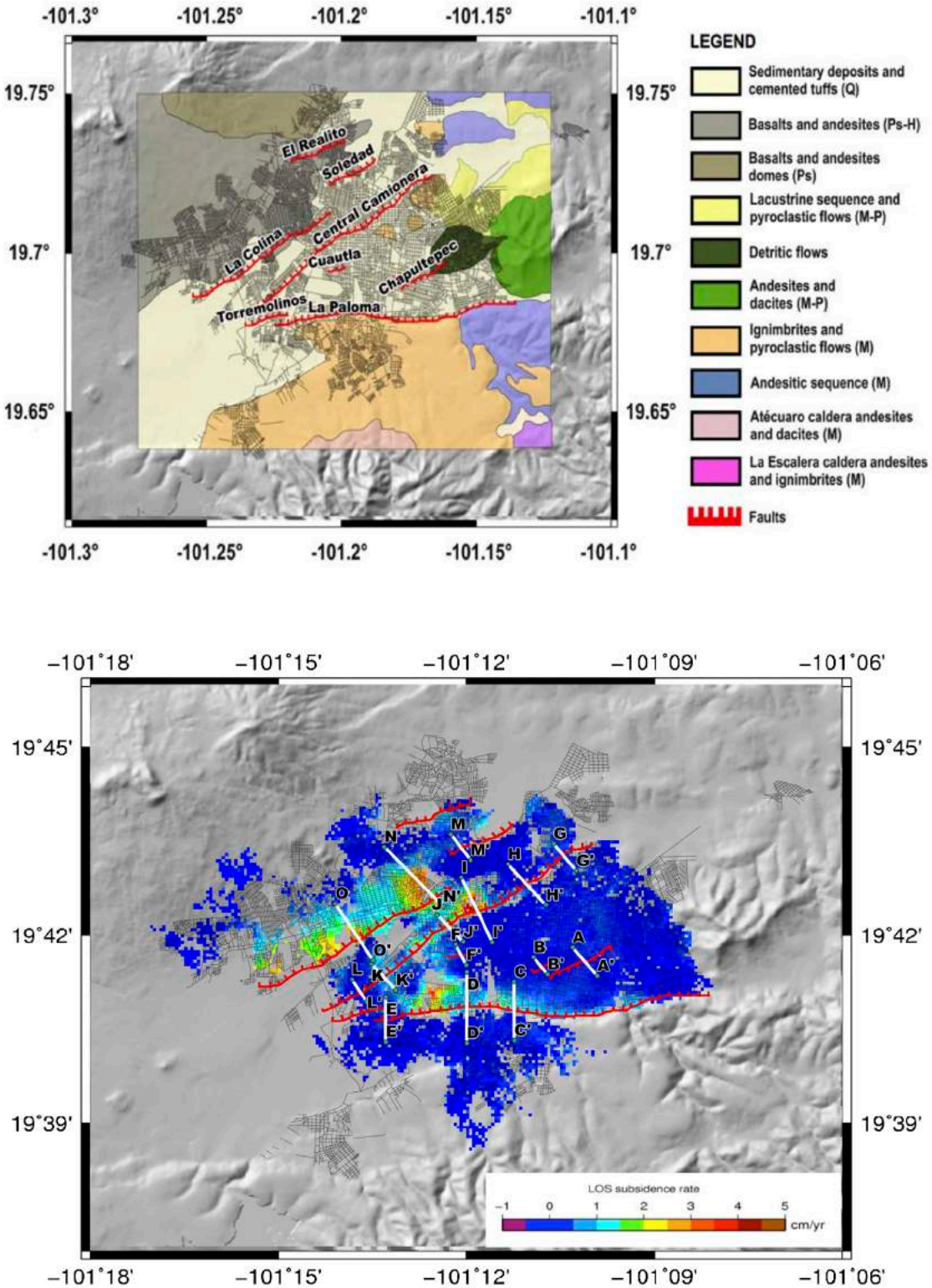

Figure 4. The maps show the average annual rate of subsidence along the Line of Sight (LOS) of the satellite: 4a) During the period July 2003 – January 2007; and 4b) from December 2008 to September 2010.

of the ground deformation (*e.g.,* López-Quiroz, 2008). All the cross sections and time series calculated are shown in the Electronic Supplement to this paper. In the discussion, we select some relevant examples to illustrate and discuss the observations.

Deformation in the vicinity of La Paloma fault

Three cross sections were calculated across the La Paloma fault (Sections CC', DD' and EE' on Figures 4a and 4b). Also, subsidence time histories were estimated for representative locations near the fault (points D, E, F, and G on Figure 5). Points D and E show that the hanging wall of La Paloma fault, on the Mil Cumbres Sierra, is stable in the seven-year period observed by the data. In these two points the rate of deformation is less than 1 mm/yr (see Electronic Supplement). Immediately to the north of point E, point G shows a rate of subsidence of approximately 0.7 cm/yr (Figure 6). This rate of subsidence is maintained consistently throughout the seven years covered in this study. Point F, in the western end of La Paloma fault shows a rate of subsidence of 1.8 cm/yr in the period from July 2003 to January 2007 (Figure 6); the subsidence rate later increased to 2.6 cm/yr, from December 2008 to September 2010 (Figure 6). In all cases, the subsidence of the ground behaves quasi linearly as a function of time, displaying no significant seasonal variations.

Cross sections across La Paloma fault show very different subsidence histories. Sections CC' and DD', located in the central part of La Paloma fault (Figure 4a), show an average rate of subsidence of approximately 1 cm/yr; a value similar to the subsidence rate observed in location G (see Figure 7 and Electronic Supplement). In the case of cross section EE', located in the western end of La Paloma fault, no discernible subsidence is present (Figure 7). The results of these three cross sections drawn across La Paloma fault depict the variability of ground subsidence in Morelia in different segments of the same fault.

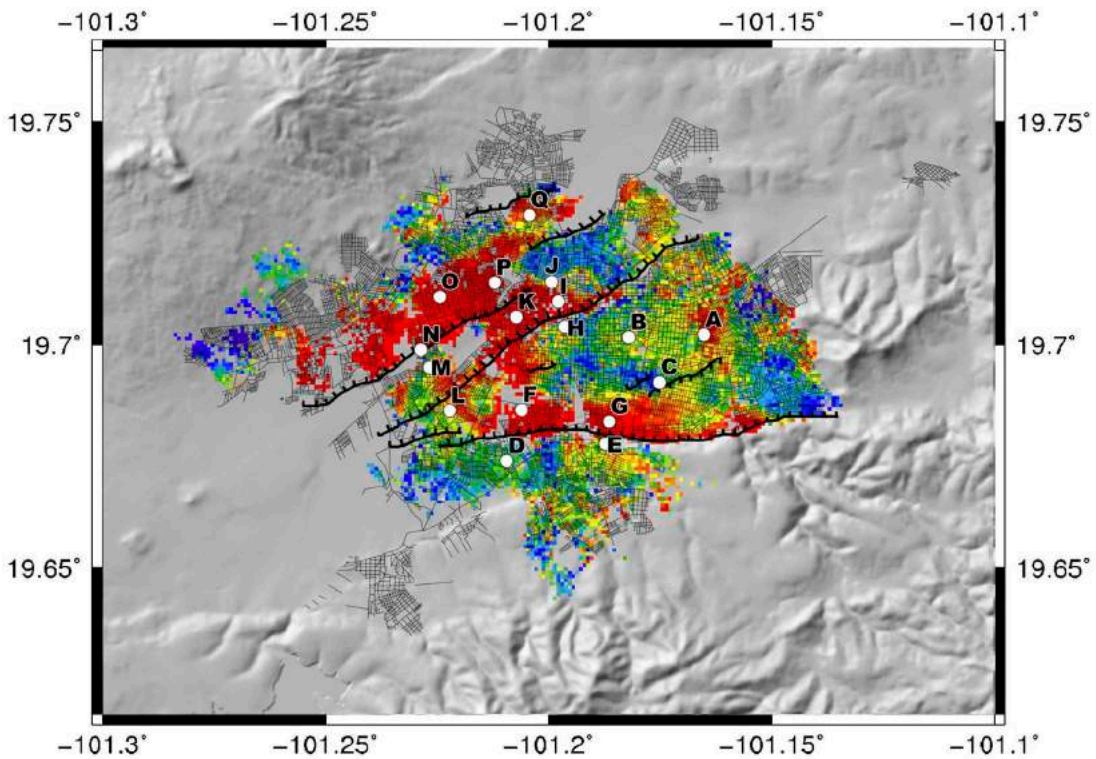

Figure 5. The map shows the location of the points in the city of Morelia for which a time series was estimated in the inversion process. The color scale indicates the correlation coefficient of the pixels used in the time series. Warm colors (red) show a high correlation and the colder tones (blue and purple) indicate areas of low correlation. The points selected to construct the time series were chosen, whenever possible, in areas of relatively large correlation.

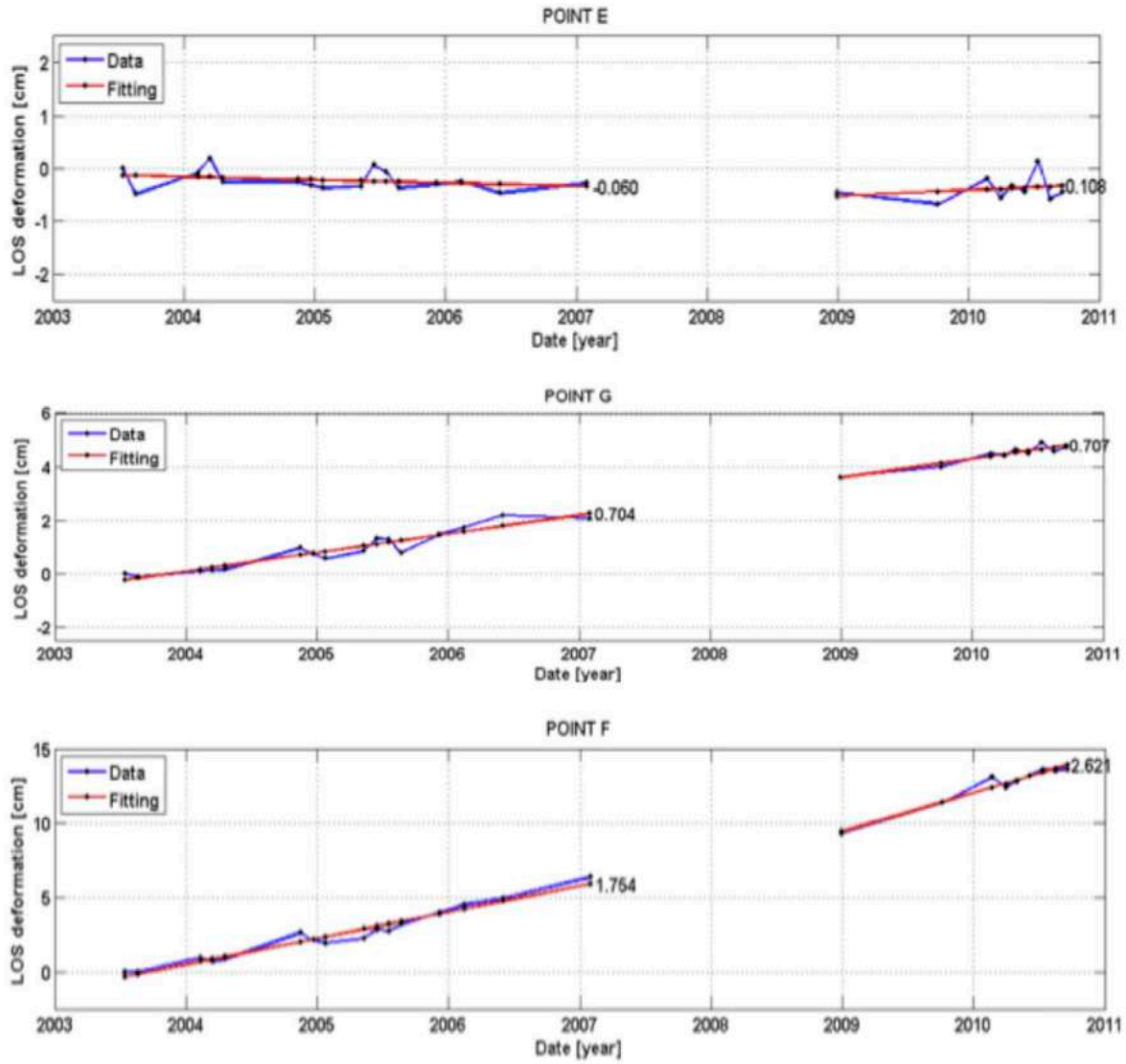

Figure 6. Time series for points E, G and F located in the vicinity of La Paloma fault (Figures 1 and 4). The solid blue line indicates the ground deformation estimated from the inversion process of the InSAR images in Line of Sight (LOS) of the satellite. The solid red line indicates the best linear fit of the deformation model; the numbers indicate the average annual subsidence rate.

Subsidence near Central Camionera fault

Subsidence time histories were estimated for several locations and for six cross sections in the vicinity of the Central Camionera fault. As in the case of La Paloma fault, the cross sections indicate great variability of the ground subsidence rates along the strike of the fault (see the Electronic Supplement). Point H lies on the hanging wall of the Central Camionera fault and shows no appreciable subsidence during the time covered (Figure 8). The area called Prados Verdes (point I on Figure 5) is on the footwall of the fault. This area shows the largest ground subsidence rate observed in the city (Figure 8). During the first period of observation, point I shows a relatively low rate of subsidence (Figure 8). During this time, the water well located in the vicinity of this area was not operational due to the installation of new casing. The bore diameter was increased from 96 to 102 m (Cigna *et al*., 2012). The drastic increase of subsidence, going from 1.2 to 4.4 cm/yr during the second observational period (Figure 8), is presumably related to the increase of the water extraction rate and a

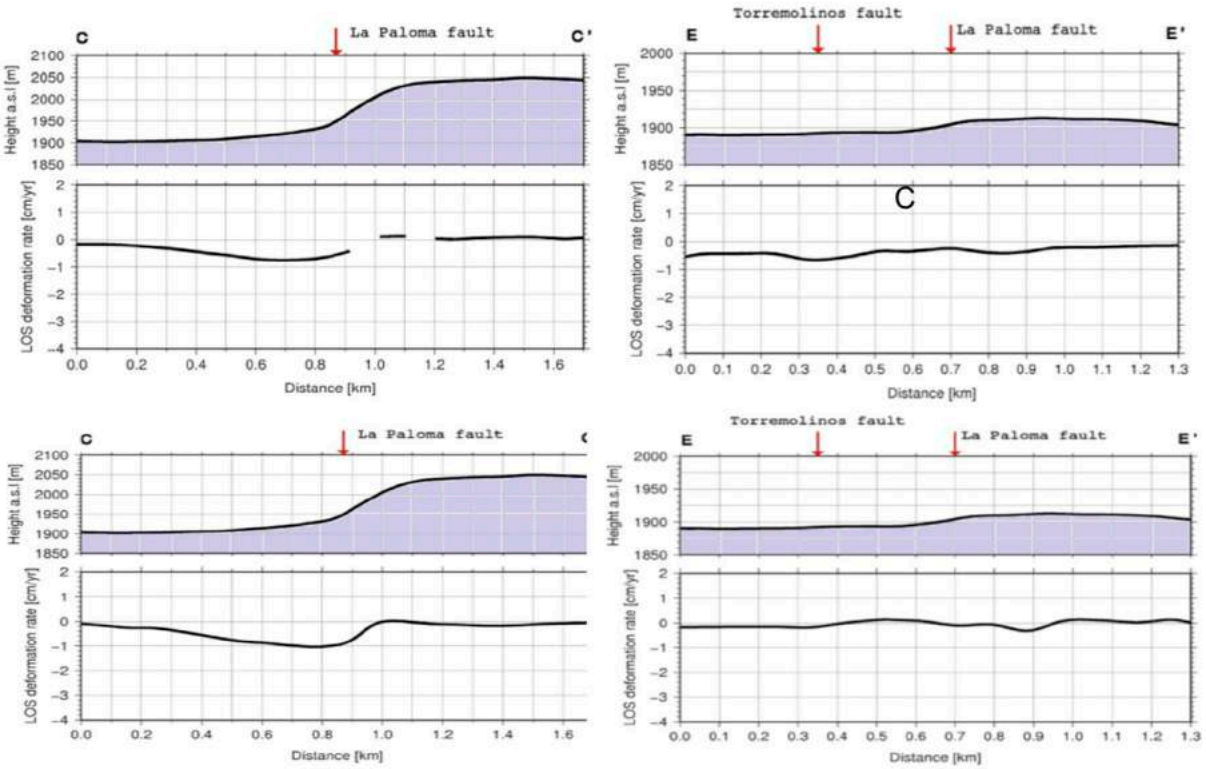

Figure 7. Cross sections CC´and DD´ across La Paloma fault as shown on Figure 4. The topography is shown on top and the deformation of the ground estimated from InSAR is shown at the bottom. The upper image of each cross section depicts the period from 2003 to 2007; the lower pane reflects deformation from 2008 to 2010.

further reduction of the static level of the well (Cigna *et al*., 2012). To the west of the Prados Verdes area, point K, also on the footwall of the Central Camionera fault, shows a stable and linear rate of subsidence of approximately 1 cm/yr.

Six cross sections were calculated across the Central Camionera fault. In the central part of the fault, on cross section II', there is a clear change in the subsidence rate on both sides of the fault. Along this cross section, the variation in the rates of subsidence, observed also in point I, is clearly evident (Figure 9). This rapid change in the rate of subsidence is probably due also to the increase in production of Prados Verdes well. In the eastern part of the fault (Section HH') there is no discernable ground deformation during the seven years of the study (Figure 9). A similar result is observed also in cross section LL' (see the Electronic Supplement). The gaps observed in cross sections HH´and II´ are due to points on the ground where coherence was lost and where the RMS values were above the prescribed levels of quality.

Subsidence in the footwall of La Colina fault

In the area near La Colina fault, several locations were selected to calculate the variation of subsidence as a function of time. Points N and P, on the hanging of the fault, show a very similar subsidence behavior. In the first three years of observation, the subsidence in both cases ranged from 1.7 cm/yr in Point N, to 1.8 cm/yr in Point P (Figure 10). From 2009 to 2010, the subsidence rate increased to almost 3 cm/yr in point P and to 2 cm/yr in Point N, again showing an increase in the subsidence rate of the ground in the second period studied. In all cases, however, the behavior is linear, showing no temporal or seasonal variations. Point O is also in the footwall of La Colina Fault. However, this location is farther away from the fault trace than points N and P. The average rate of subsidence is slower than in the previous two locations, showing an average subsidence of between 0.6 and 0.8 cm/yr (Figure 10).

Two cross sections were calculated crossing La Colina fault (cross sections NN' and OO´ (Figure 11). Cross sections NN´ and OO´ show

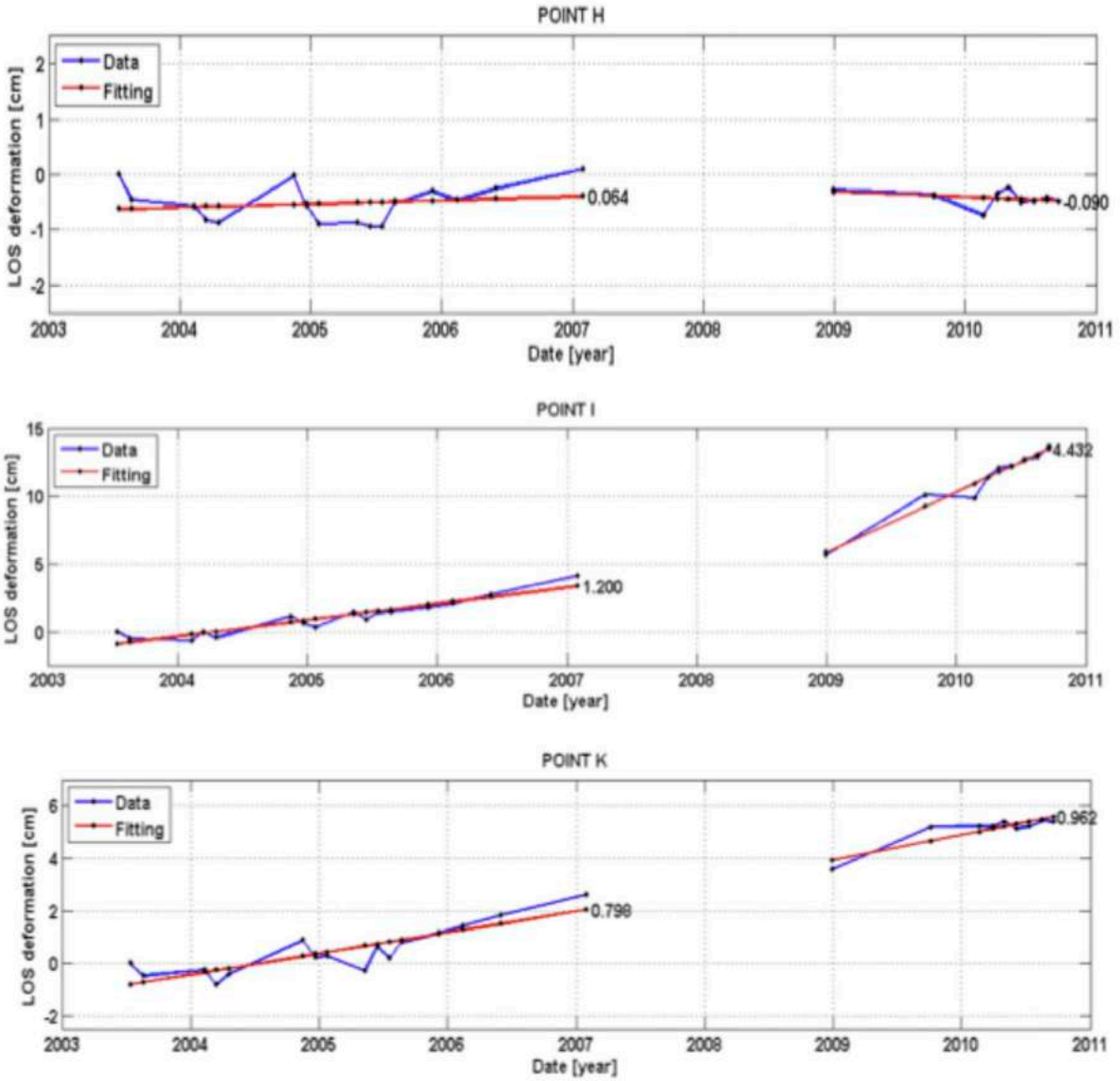

Figure 8. Time series for points H, I and K located in the vicinity of the Central Camionera fault (Figure 5). The solid blue line indicates the ground deformation estimated from the inversion process of the InSAR images in Line of Sight (LOS) of the satellite. The solid red line represents the best linear fit of the deformation model; the numbers indicate the average annual subsidence rate.

subsidence of the ground to the north of the surface expression of La Colina fault. In both cases, a broad area subsides at a maximum rate of approximately 2 to 2.5 cm/yr. The deformation of the ground stops to the north of the city, where the Pliocene basalt and andesite deposits delineate the northern boundary of the Morelia basin (Figure 11). The deformation rate on these two cross sections remains constant during the two periods studied. In both cases, some coherence is lost in the central part of the cross sections.

Summary and conclusions

A new analysis of ground subsidence in the city of Morelia, in central Mexico, is presented using the small baselines methodology to estimate interferograms. The purpose of this work is to extend the work done by Cigna *et al*. (2011; 2012) in mapping the ground subsidence in the city. The identification of the areas of the city where subsidence occurs and the estimation of subsidence rates in various locations is important to mitigate and predict the locations

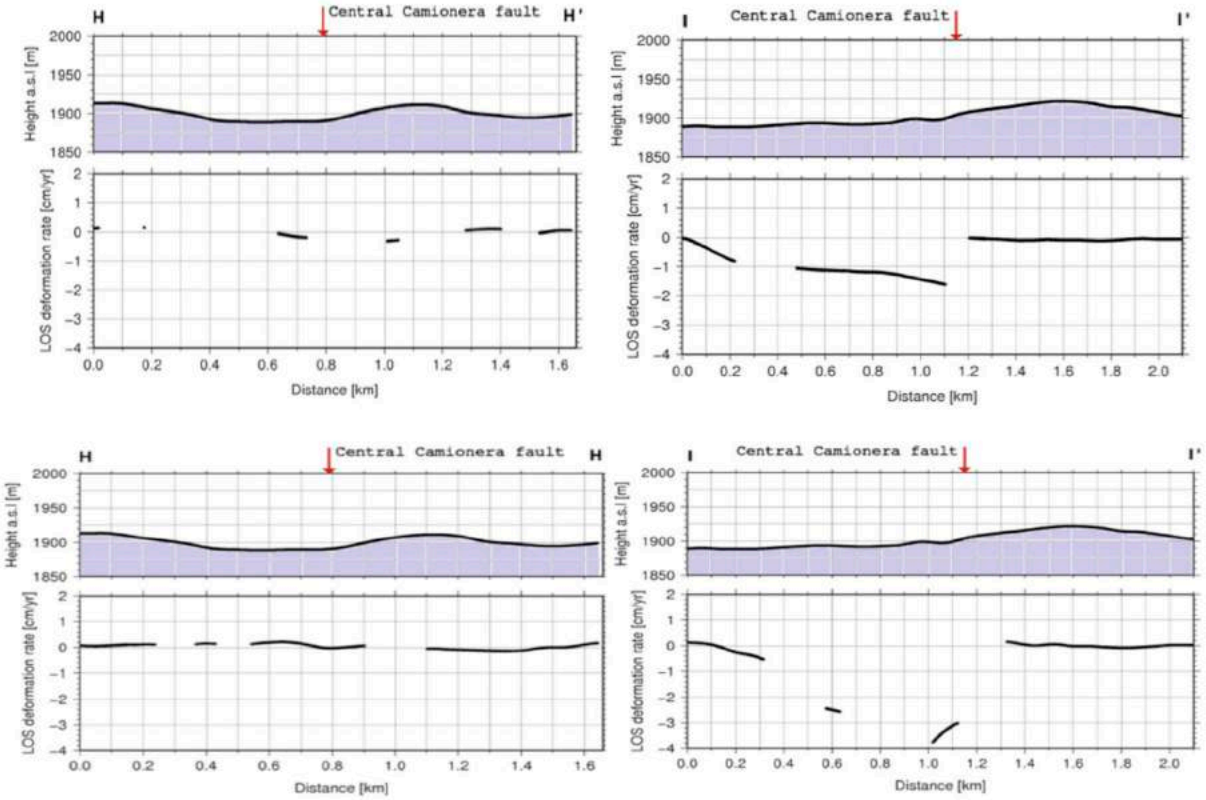

Figure 9. Cross sections HH´ and II´ across the Central Camionera fault as shown on Figure 4a. The topography is shown on top and the deformation of the ground estimated from InSAR is shown at the bottom. The upper image of each cross section depicts the period from 2003 to 2007; the lower pane reflects deformation from 2008 to 2010.

of the city that will be more prone to damage and ground faulting in the future.

From a regional point of view, most of the city of Morelia shows no significant subsidence. In fact, there is no deformation observed on many of the mapped faults, such as the Chapultepec, Cuautla and Torremolinos. The subsidence evidenced by the InSAR observations is concentrated in the western half of the city and along three major faults: La Paloma, Central Camionera and La Colina. However, the ground deformation is not continuous and homogeneous along these faults. Subsidence takes place only on specific locations along the footwall of these three faults. La Colina fault is the one that exhibits a more continuous deformation of the ground along strike.

The largest subsidence rate of 4 cm/yr is observed to the north of the central part of the Central Camionera fault. This region showed a rapid increase in subsidence from 2009 to 2010, probably due to the increased flow of Prados Verdes well. In general, however, there is no direct correlation between the rates of water extraction and the areas of larger subsidence. In the same manner, as observed by Cigna *et al*. (2012), there is no clear correlation between the thickness of the Quaternary sediments in different parts of the Morelia basin and the rate of subsidence.

Garduño Monroy *et al*. (2001) suggested that the ground deformation in the city of Morelia is the surface expression of motion on subsurface basement faults. These authors suggest that these buried faults are continuously deforming by aseismic creep. These authors attribute the presence of surface deformation of the ground as a reflection of the motion on basement faults beneath the sediments, caused by creep at depth. However, the rates of subsidence observed on the ground are of several cm/yr. The rates of subsidence observed in Morelia

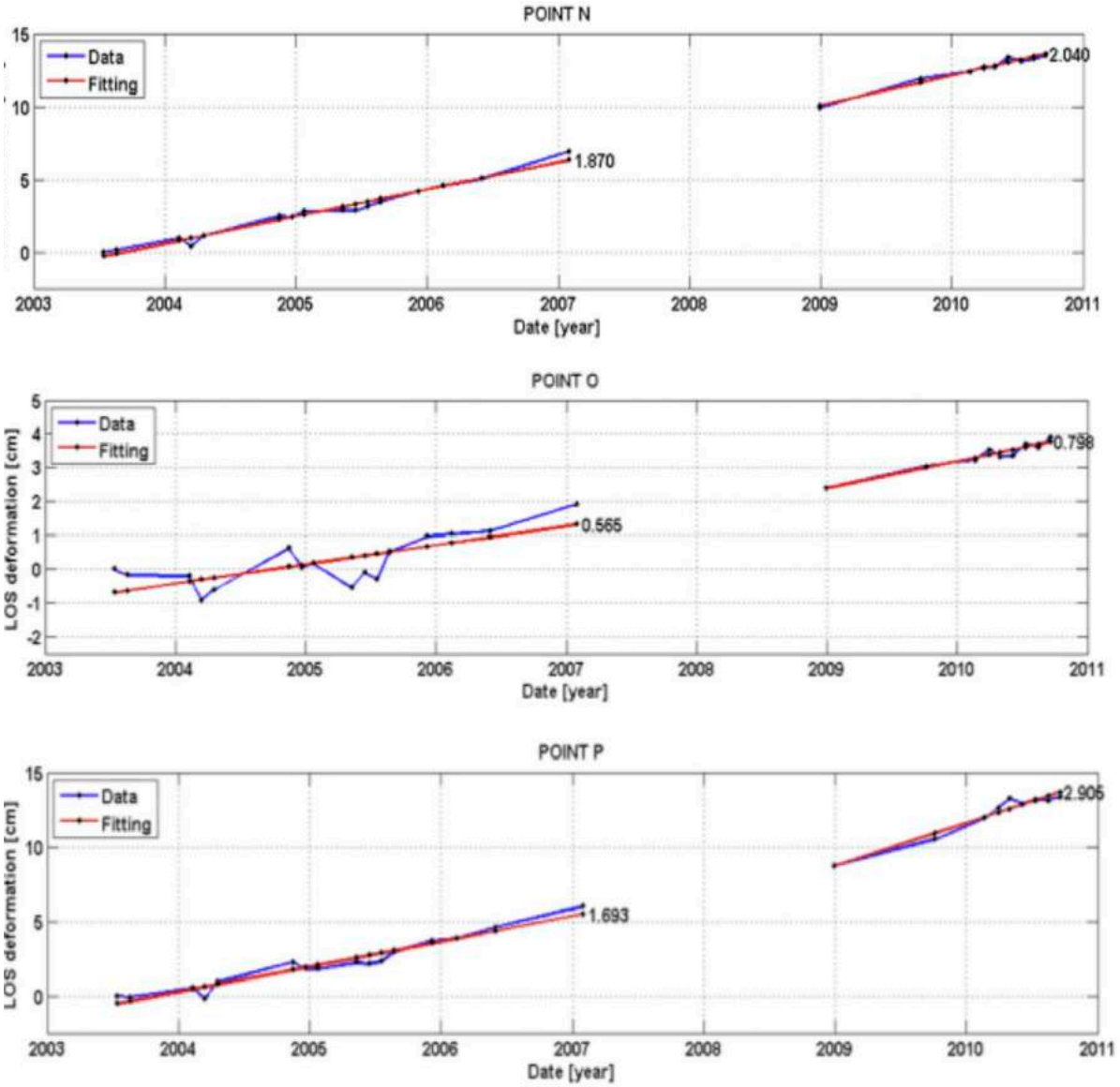

Figure 10. Time series for points N, O and P located in the vicinity of La Colina fault (Figure 5). The solid blue line indicates the ground deformation estimated from the inversion process of the InSAR images in Line of Sight (LOS) of the satellite. The solid red line indicates the best linear fit of the deformation model; the numbers indicate the average annual subsidence rate.

are almost an order of magnitude larger than creep deformation measured on active faults. For example, fault creep observed on San Andreas is in the order of mm/yr (*e.g.,* Schulz *et al.*, 1982; Lienkaemper *et al*., 2001; Lyons and Sandwell, 2003). Thus slow aseismic creep motion on subsurface faults would not explain the large subsidence rates observed in the Morelia basin.

The ground subsidence observed in the city of Morelia is highly variable in areal extent and concentrated in specific areas. The lack of direct correlation between subsidence of the ground and water extraction and the thickness of the sediments suggests that the deformation of the ground is due to the preexisting topography of the basement that controlled the complex depositional history of volcanic and lacustrine deposits in the Morelia basin. This poses a challenge to manage the exploitation of the aquifer in order to minimize and control the ground deformation.

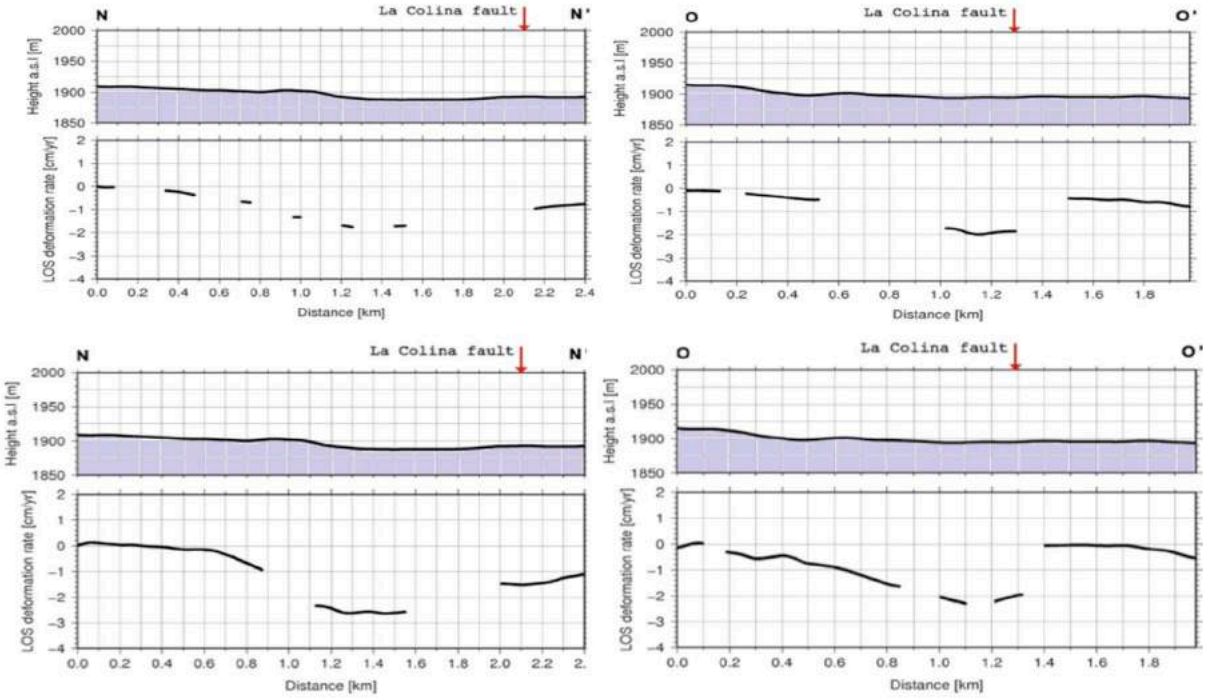

Figure 11. Cross sections NN´and OO´ across La Colina fault as shown on Figure 4a. The topography is shown on top and the deformation of the ground estimated from InSAR is shown at the bottom. The upper image of each cross section depicts the period from 2003 to 2007; the lower pane reflects deformation from 2008 to 2010.

References

Aguirre-Díaz, G. J., Zúñiga-Dávila- Madrid, F. R., Pacheco-Alvarado.F. J., Guzmán-Speziale, M., and Nieto-Obregón, J., 2000. El graben de Querétaro, México. Observaciones de fallamiento activo. *GEOS,* 20, 1, 2-7.

Amelung, F., Galloway, D. L., Beii, J. W., Zebker, H. A., and Laczniak, R. J., 1999. Sensing the ups and downs of Las Vegas: InSAR reveals structural control of land subsidence and aquifer-system deformation. *Geology,* 27, 6, 483-486.

Arreygue-Rocha, E., Garduño-Monroy, V. H., Canuti, P., Casagli, N., Lotti, A., and Chiesa, S., 2002. Análisis geomecánico de la inestabilidad del escarpe La Paloma en la Ciudad de Morelia, Michoacán, México. *Revista Mexicana de Ciencias Geológicas,* 19, 2, 91-106.

Arreygue-Rocha, E., Garduño-Monroy, V. H., Canuti, P., Casagli, N., and Lotti, A., 2005. Riesgos geomorfólogicos e hidrológicos en la Ciudad de Morelia, Michoacán, México. *Geotermia,* 18, 1, 26-35.

Ávila-Olvera, J. A., and Garduño-Monroy, V. H., 2006. Hundimientos ocasionados por Procesos de Subsidencia-Creep-Falla (PSCF) en la ciudad de Morelia, Mich., México. *Geotermia,* 19, 2, 50-59.

Ávila-Olvera, J. A., 2008. Evolución de los procesos de subsidencia-creep-falla, casos: Morelia, Mich. and Celaya, Gto. UNAM, Tesis, 249 pp.

Ávila-Oiivera, J. A., and Garduño-Monroy, V. H., 2008. A GPR study of subsidence creep-fault process in Morelia, Michoacán, Mexico. *Engineering Geology,* 100,69-81.

Ávila-Olvera, J. A., Farina, P., and Garduño-Monroy, V. H., 2010. Land subsidence monitored by satellite interferometry in Mexican cities. *IAHS Pub.* 339, 316-318.

Berardino, P., Fomaro, G., Lanari, R., and Sansosti, E., 2002. A new algorithm for surface deformation monitoring based on Small Baseline differential SAR Interferograms. *IEEE Transactions on Geoscience and Remote Sensing,* 40, 11, 2375-2383.

Buckley, S. M., Rosen, P. A., Hensley, S., and Tapley, B. D., 2003. Land subsidence in Houston, Texas, measured by radar interferometry and constrained by extensometers. *Journal of Geophysical Research,* 108,811, 2542, 1-18.

Cabral-Cano, E., Dixon, T. H., Miralles-Wilhelm, F., Diaz-Molina, O., Sánchez-Zamora, 0., and Carande, R. E., 2008. Space geodetic imaging of rapid ground subsidence in Mexico City. *Geological Socíety of America Bulletin,* 120, 1556-1566.

Cabral-Cano, E., Arciniega-Ceballos, A., Díaz-Molina, O., Cigna, F., Ávila-Oiivera, A., Osmanoglu, B., Dixon, T., DeMets, C., Garduño-Monroy, V. H., Vergara-Huerta, F., and Hernández-Quintero, J. E., 2010. Is there a tectonic component to the subsidence process in Morelia, Mexico?, *IAHS Publication* 339, 164-169.

Calderhead A., Therrien, R., Rivera, A., Martel, R., and Gañias, J., 2011. Simulating pumping-induced regional land subsidence with the use of lnSAR and field data in the Toluca Valley, Mexico. *Advances in Water Resources,* 34, 83-97.

Carreón-Freyre, 0., and Cerca, M., 2006. Delineating the near-surface geometry of the fracture system affecting the Valley of Querétaro, Mexico: Correlation of GPR signatures and physical properties of sediments. *Near Surface Geophysics,* 49-55.

Carreón-Freyre, D., Hidalgo-Moreno, C.M., and Hemández-Marín, M., 2006. Mecanismos de fracturamiento de depósitos arcillosos en zonas urbanas. Caso de deformación diferencial en Chalco, Estado de México. *Boletín de la Sociedad Geológica Mexicana,* Número Especial de Geología Urbana, LVIII, 2, 237-250.

Carrillo, N., 1948. lnfluence of artesian wells on the sinking of México City, in Volume: Nabor Carrillo, "El hundimiento de la Ciudad de México y el Proyecto Texcoco. Comisión Impulsora y Coordinadora de la Investigación Científica Anuario 47: 7-14.

Castañeda, M. H., Murillo-Méndez, M. A., Fuentes-López, *J.* A., and Monsiváis-Santoyo, J. P., 1993. Levantamiento cartográfico de las fallas y facturas geológicas de la ciudad de Aguascalientes. *Revista Investigación y Ciencia de la UAA,* 9, 43-47.

Castañeda, M. H., Murillo-Méndez, M. A., Fuentes-López, J. A., and Monsiváis-Santoyo, J. P., 1995. Comentarios al estudio de fallas y fracturas geológicas de la ciudad de Aguascalientes. Mecanismo de fracturamiento. *Revista Investigación y Ciencia de la UAA,* 14, 40-43.

Cavalié. 0., Doin, M. P., Lasserre, C., and Briole, P., 2007. Ground motion measurement in the Lake Mead area, Nevada, by differential synthetic aperture radar interferometry time series: probing the lithosphere rheological structure. *Journal of Geophysical Research,* 112, 803403, 1-18.

Chai, J . C., Shen, S. L., Zhu, H. H., and Zhang, X. L., 2004. Land subsidence due to groundwater drawdown in Shanghai. *Géotechnique,* 54, 2, 143-147.

Chaussard, E., Wdowinski, S., Cabral-Cano and E., Amelung, F., 2014, Land subsidence in central Mexico detected by ALOS InSAR time-series, *Remote Sensing of Environment*, 140, 94-106, ISSN 0034-4257, https://doi.org/10.1016/j.rse.2013.08.038.

Chávez-Alegría, 0., 2008. Modelación física experimental del fenómeno de subsidencia. Universidad Autónoma de Querétaro. Tesis, 151 pp.

Cigna, F., Cabral-Cano, E., Osmanoglu, B., Dixon, T. H., and Wdowinski, S., 2011. Detecting subsidence-induced faulting in Mexican urban areas by means of persistent scatterer interferometry and subsidence horizontal gradient mapping. *IGARSS,* 2125-2128.

Cigna, F., Osmanoglu, B., Cabral-Cano, E., Dixon, T. H., Ávila-Olivera, J. A., Garduño-Monroy, V. H., DeMets, C., and Wdowinski, S., 2012. Monitoring land subsidence and its induced geological hazard with Synthetic Aperture Radar lnterferometry: A case study in Morelia, Mexico. *Remote Sensing of Environment,* 117, 146-161.

Dehghani, M., Zoej, M. J. V., Entezam, Mansourian, A., and Saatchi, S., 2009. lnSAR monitoring of progressive land subsidence in Neyshabour, northeast Iran. *Geophys. J. lnt.,* 178, 47-56.

Ding, X. l., Liu, G.X., Li, Z.W., Li, Z.L and Chen, Y. Q., 2004. Ground subsidence monitoring in Hong Kong with satellite lnterferometry. *Photogrammetric Engineering and Remote Sensing,* 70, 10, 1151-11156.

Esquivel, R. R., 2009. Análisis y modelado de deformaciones locales de la corteza terrestre con radar de apertura sintética y datos geodésicos. Tesis, UNAM, 105 pp.

Farina, P., Ávila-Olivera, J. A., and Garduño-Monroy, V. H., 2007. Structurally-controlled urban subsidence along the Mexican volcanic belt (MVB) monitored by lnSAR. *Envisat Symposium.* Montreux, Switzerland.

Farina, P., Avila-Olivera, J. A., Garduño-Monroy, V. H., and Catani, F., 2008. DlnSAR analysis of differential ground subsídence affecting urban areas along the Mexican Volcanic Belt (MVB). *Rivista italiana di Telerilevamento,* 40(2), 103-113.

Farr, T. G., and Kobrick, M., 2000. Shuttle Radar Mission produces a wealth of data. *American Geophysical Union, EOS*, 81,48, 583-585.

Ferreti, A., Pratti, C., and Rocca, F., 2000. Nonlinear subsidence rates estimation using permanent scatters in differential SAR interferometry. *IEEE Transactions on Geosciences and Remote Sensing,* 39 (5), 2202-2212.

Ferretj A., Pratti, C., and Rocca, F., 2001. Permanent Scatterers in SAR lnterferometry. *IEEE*, *Transactions Geosciences and Remote* Sensing, 39, 1, 8-20.

Garduño-Monroy, V. H., Arreygue-Rocha, E., lsrade-Aicántara, and Rodrlguez-Torres, G. M., 2001. Efectos de las fallas asociadas a la sobrexplotación de acuíferos y la presencia de fallas potencialmente sísmicas en Morelia, Michoacán, México. *Revista Mexicana de Ciencias Geológicas,* 18, 37-54

Gayol, R., 1925. Estudio de las perturbaciones que en el fondo de la Ciudad de México ha producido el drenaje de las aguas del subsuelo, por las obras del desagüe y rectificación de los errores a que ha dado lugar una incorrecta interpretación de los efectos producidos: *Revista Mexicana de Ingeniería y Arquitectura,* v. 111, 96-132.

Goldstein, R. M. and Wemer, C. L., 1998. Radar interferogram filtering for geophysical applications. *Geophysical Research Letters,* 25, 21,4035-4038.

Goldstein, R.M., Zebker, H.A., and Wemer, C. L., 1988. Satellite radar interferometry: Two-dimensional phase unwrapping. *Radio Science,* 23, 4, 713-720.

Hanssen, R. F., 2001. Radar interferometry: data interpretation and error analysis. *Kluwer Academíc Publíshers,* 308 pp.

Le Mouélic, S., Raucoules, D., Carmec, C., and King, C., 2005. A Least Squares adjustment of multi-temporal lnSAR data: Application to the ground deformation of Paris. *Photogrammetric Engineering and Remote Sensing,* 17, 2, 197-204.

Lienkaemper, J. J., Galehouse, J. S. and Simpson, R. W. (2001). Long-term monitoring of creep rate along the Hayward fault and evidence for a lasting creep response to 1989 Loma Prieta earthquake. *Geophys. Res. Lett*, *28*(11), 2265-2268.

López-Doncel, R., Mata-Segura, J. L., Cruz-Márquez, J., Arzate-Fiores, J., and Pacheco-Martínez, J., 2006. Riesgo geológico para el patrimonio histórico. Ejemplos del centro histórico de la ciudad de San Luis Potosí. *Boletín de la Sociedad Geológica Mexicana,* Número Especial de Geología Urbana, LVIII, 2, 259-263.

López-Quiroz, P., 2008. Séries temporelles de la subsidence de la ville de Mexico obtenues par interférométrie radar. TELECOM, ParisTech, Tesis doctoral, 140 pp.

López-Quiroz, P., Doin, M. P., Tupin, F., Briole, P., and Nicolas, J. M., 2009. Time series analysis of Mexico City subsidence constrained by radar interferometry. *Journal of Applied Geophysics,* 69, 1-15.

Lu, L., and Liao, M., 2008. Subsidence measurement with PS-InSAR techniques in Shanghai urban. *The Intematíonal Archives of the Photogrammetry, Remote Sensing and Spatial lnformation Science,* XXXVII, 173-178.

Lyons, S. and Sandwell, D. (2003). Fault creep along the southern San Andreas from interferometric synthetic aperture radar, permanent scatterers, and stacking. *Journal of Geophysical Research: Solid Earth*, *108*(B1).

Marfai, M. A., and King, L., 2007. Monitoring land subsidence in Semarang, Indonesia. *Environmental Geology.,* 53, 651-659.

Mejía-Gómez, J. A., and Sandoval-Minero, R., 2004. Uso del agua subterránea en la region acuífera lrapuato-Valle de Santiago (México) y su impacto sobre el sistema hidrogeológico. *Boletín Geológico y Minero,* 115, 311-318.

Ortega-Guerrero, A., Cherry, J. A., and Rudolph, D. L., 1993. Large-Scale Aquitard Consolidation near, Mexico City. *Ground Water,* 31, 5, 708-718.

Osmanoglu, B., Dixon, T. H., Wdowinski, S., Cabral-Cano, E., and Jiang, Y., 2011. Mexico City subsidence observed with persistent scatterer lnSAR. *International Journal of Applied Earth Observation and Geoinformation,* 13. 1-12.

Pacheco-Martínez, J., 2007. Modelo de subsidencia del valle de Querétaro y predicción de agrietamientos superficiales. UNAM, Tesis, 224 pp.

Pacheco-Martínez, J., and Arzate-Flores, J., 2007. Análisis multicapa de la subsidencia en el Valle de Querétaro, México. *Revista Mexicana de Ciencias Geológicas,* 24, 3, 389-402.

Pacheco-Martínez, J., Arzate, J., Rojas, E., Arroyo,M., Yutsi, V., and Ochoa, G., 2006. Delimitation of ground failure zones due to land subsidence using gravity data and finite element modeling in the Querétaro valley, México. *Engineering Geology,* 84, 143-160.

Poland, J. F., 1984. Guidebook to studies of land subsidence due to groundwater withdrawal, prepared for the International Hydrogeological Programme, Working Group 8.4. UNESCO, Book Crafters, Chelsea, Massachusetts.

Rosen, P.A., Hensley, S., Peltzer, G., and Simons, M., 2004. Updated repeat orbit interferometry package released. *EOS Transactions AGU*, 85, 5, 47.

Schmidt, D. A., Bürgmann, R., 2003. Time-dependent land uplift and subsidence in the Santa Clara valley, California, from a large interferometric synthetic aperture radar data set. *Journal of Geophysical Research*, 108, 89, 2416, 1-13.

Schroeder-Aguirre, A. A., 2010. Análisis de la deformación del fallamiento por subsidencia en la zona de lrapuato, Gto, UNAM, Tesis, 111 pp.

Schulz, S. S., Mavko, G. M., Burford, R. O., and Stuart, W. D. (1982). Long-term fault creep observations in central California. *Journal of Geophysical Research: Solid Earth*, 87(B8), 6977-6982.

Stramondo, S., Bozzano, F., Marra, F., Wegmüller, U., Cinti, F. R., Moro, M., and Saroli, M., 2008. Subsidence induced by urbanization in the city of Rome detected by advanced lnSAR technique and geotechnical investigations. *Remote Sensing of Environment*, 112, 3160-3172.

Strozzi, T., and Wegmüller, U., 1999. Land subsidence in Mexíco City mapped by ERS Differential SAR lnterferometry. Geoscience and Remote Sensing Symposium. /GARSS'99 Proceedings, IEEE, 4, 1940-1942.

Strozzi, T., Wegmüller, U., Tosi, L., Bitell, G., and Spreckels, V., 2001. Subsidence monitoring with differential SAR lnterferometry. Photogrammetric Engineering and Remote Sensing, 67, 11, 1261-1270.

Trujillo-Candelaria, J. A., 1989. Fallamientos de terrenos en Celaya, Gto. Academia Mexicana de Ingeniería. *Alternativas Tecnológicas*, 29, 367-369.

Trujillo-Candelaria, J.A., 2009. Fallamientos de terrenos por sobrexplotación de acuíferos en Celaya, Gto., Aquaforum, 52, 24-27.

Usai, S., 2003. A least squares database approach for SAR lnterferometric data. *IEEE Transactíons on Geoscience and Remote Sensing*, 41, 4, 753-760.

Vargas, R. M. V., 1999. La subsidencia y su problemática en la ciudad de Celaya, Guanajuato. UNAM, Tesis, 144 pp.

Vilardo, G., Ventura,G., Terranova, C., Matano, F., and Nardó, S., 2009. Ground deformation due to tectonic, hydrothermal, gravity hydrogeological and anthropic processes in the Campania Region (Southem ltaly from Permanent Scatterers Synthetic Aperture Radar lnterferometry, *Remote Sensing of Envíronment*, 113, 197-212.

Watson, K. M., Bock, Y., and Sandwell, D. T., 2002. Satellite interferometric observations of displacements associated with seasonal groundwater in the Los Angeles basin. *Journal of Geophysical Research*, 107, B4, 1-17.

Yan, Y., López-Quiroz, P., Doin, M. P., Tupin, F., and Fruneau, B., 2009. Comparison of two methods in multi-temporal differential SAR Interferometry: Application to the measurement of Mexico City subsidence. MultiTemp 2009 -The Fifth International Workshop on the Analysis of Multi-temporal. Remote Sensing Images, Groton, Connecticut.

Zermeño de León, M. E., Mendoza-Otero, E., y Calvillo-Silva, G., 2004. Medición del hundimiento y modelo para estudiar el agrietamiento de la ciudad de Aguascalientes. Revista Investigación y Ciencia de la UAA, 31, 35-40.

Zermeño de León, M. E., Esquivel-Ramírez, R., Hemández-Navarro, A., Mendoza-Otero, E., and Arellano-Sánchez, J., 2005. Influencia de la extracción del agua en la subsidencia y agrietamiento de la ciudad de Aguascalientes. *Revista Investigación y Ciencia de la UAA*, 32, 15-22.

Appendix A

Orbital and stratified atmospheric correction:

Equation 1 was adjusted (Cavalié *et al*., 2007; López-Quiroz *et al*., 2009):

$$\phi_0 = (ax+b)y + cx + d + \phi z \text{ for } z > 1930m \quad (1)$$

where a, b, c, $d\phi$ are obtained using least square minimization. And z is the elevation where the deformation is concentrated and obtained by permorfing a linear regression between the interferometric phase and the elevation.

Inversión process

The phase delay time series were obtained using a least squares inversion (Cavalié *et al*., 2007) solving the linear equation:

$$d_l = G_l\, m_l \quad (2)$$

where, d_l is the vector including the data of interferometric phase from N_l interferograms for pixel, l; m_l, is a vector including the phase delay increments between two successive images; G_l is a matrix of zeros and ones, constructed based on the fact that the phase of an interferogram (ϕ_{ij}^l), is the sum of the successive phase delays between images i and j:

$$\phi_{ij}^l = \sum_{k=i}^{j-1} m_k^l \quad (3)$$

RMS estimate in the case of pixels (Cavalié *et al*., 2007):

$$\phi RMS_{pixel}^l = \frac{1}{N_l} \sum N_l \left(\phi_{ij}^l - \sum_{k=i}^{j-1} m_k^l \right)^2 \quad (4)$$

RMS of each interferogram (Cavalié *et al*., 2007):

$$\phi_{RMS_{ifg}}^{ij} = \frac{1}{p} \sum l \left(\phi_{ij}^l - \sum_{k=i}^{j-1} m_k^l \right)^2 \quad (4)$$